Contribution from the Department of Chemistry,
University of Houston, University Park, Houston, Texas 77004

Ligand-Induced Scission of Polyhedral Clusters. Synthesis, Structures, and Reactivity of Fluorodiphosphine-Substituted Bis(arylphosphido)-Capped Tetracobalt Carbonyl Complexes

M. G. Richmond and J. K. Kochi*

Received July 31, 1986

The tetracobalt cluster $Co_4(CO)_{10}(\mu_4\text{-}PPh)_2$ (I) liberates carbon monoxide upon exposure to the difunctional fluorophosphine $(F_2P)_2NMe$ at 60 °C and produces the *tetrakis* derivative $Co_4(CO)_3(PPh)_2[(F_2P)_2NMe]_4$ (II) in excellent yields. Despite varied attempts to detect intermediates in the multiple substitution of seven CO ligands, including reactions of I with less than 1 mol of $(F_2P)_2NMe$, II is the only observable species in the thermal process. However, the monosubstituted derivative $Co_4(CO)_8(\mu_4\text{-}PPh)_2[(F_2P)_2NMe]$ (IV) is obtained in 60% yield by ligand substitution of the electrogenerated anion I^-. Cluster II crystallized in the monoclinic space group $C2/c$ with lattice constants a = 12.184 (5) Å, b = 32.890 (11) Å, c = 11.650 (5) Å, β = 111.60 (3)°, and Z = 4. The X-ray crystal structure of II indicates that the Co_4 array in I has undergone a ligand-induced scission, with a fluorodiphosphine ligand bridging the "open" side of the rectangle. Further substitution of II to the *pentakis* derivative $Co_4(CO)(PPh)_2[(F_2P)_2NMe]_5$ (III) can also be achieved by treatment with an additional 1 equiv of $(F_2P)_2NMe$ at higher temperatures (110 °C). The redox properties of II and III show reversible 0/−1 and 0/+1 couples, which generate persistent anion radicals and cation radicals, respectively. The cluster transformations as a result of multiple ligand substitutions are considered in the context of the Wade–Mingos rules as modified by Halet, Hoffmann, and Saillard.

Introduction

Polyhedral metal clusters can undergo ligand substitution with an accompanying scission of the metal–metal bonds.[1-4] Such a process formally generates coordinatively unsaturated centers at contiguous metal sites, which can serve as manifolds for multisite activation of substrates.[5-7] This potential source of coordinative unsaturation thus distinguishes metal clusters from other mononuclear organometallics and suggests that they may be appropriate models for the study of surface processes and for heterogeneous catalysts.[8]

An example of the ligand-induced cleavage of the metal–metal bond in the tetranuclear cluster $Co_4(CO)_{10}(\mu_4\text{-}PPh)_2$ by the difunctional phosphine $(F_2P)_2NMe$ was reported in a preliminary communication.[9] This tetracobalt cluster is pertinent since it can act in concert with added phosphines as a viable catalyst for the hydroformylation of olefins.[10] As such we present the details of the ligand substitution of $Co_4(CO)_{10}(PPh)_2$ (I) together with the

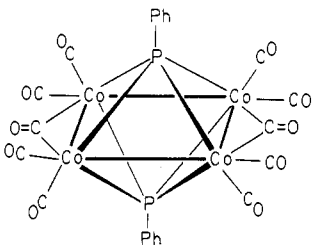

I

structural characterization and redox properties of the resultant $(F_2P)_2NMe$-substituted tetracobalt clusters. For convenience, the diphosphine $(F_2P)_2NMe$ will be referred to hereafter as the *fluorodiphosphine* ligand.

Results

I. Interaction of the Tetracobalt Cluster I with the Difunctional Fluorophosphine $(F_2P)_2NMe$. The exposure of the tetracobalt cluster I to the fluorodiphosphine ligand was carried out under three types of reaction conditions, viz. thermal, oxidative, and reductive, as described below.

A. Thermal Reactions. When a benzene solution of the tetracobalt cluster I was simply heated with 4 mol of $(F_2P)_2NMe$ at 60 °C, 7 mol of carbon monoxide was liberated, and the tetrakis

(1) (a) Huttner, G.; Schneider, J.; Muller, H. O.; Mohr, G.; Von Seyerl, J.; Wohlfahrt, L. *Angew. Chem., Int. Ed. Engl.* **1979**, *18*, 76. (b) Schneider, J.; Huttner, G. *Chem. Ber.* **1983**, *116*, 917. (c) Schneider, J.; Zsolnai, L.; Huttner, G. *Cryst. Struct. Commun.* **1982**, *11*, 1227. (d) Schneider, J.; Minelli, M.; Huttner, G. *J. Organomet. Chem.* **1985**, *294*, 75. (e) Knoll, K.; Huttner, G.; Zsolnai, L.; Jibril, I.; Wasiucionek, M. *J. Organomet. Chem.* **1985**, *294*, 91. (f) Schneider, J.; Zsolnai, L.; Huttner, G. *Chem. Ber.* **1982**, *115*, 989.

(2) (a) Field, J. S.; Haines, R. J.; Smit, D. N. *J. Organomet. Chem.* **1982**, *224*, C49. (b) Field, J. S.; Haines, R. J.; Smit, D. N.; Natarajan, K.; Scheidsteger, O.; Huttner, G. *J. Organomet. Chem.* **1982**, *240*, C23.

(3) (a) Muller, M.; Vahrenkamp, H. *Chem. Ber.* **1983**, *116*, 2311. (b) Vahrenkamp, H. *Angew. Chem., Int. Ed. Engl.* **1978**, *17*, 379. (c) Vahrenkamp, H. *Philos. Trans. R. Soc. London, A* **1982**, *308*, 17. (d) Muller, M.; Vahrenkamp, H. *Chem. Ber.* **1983**, *116*, 2322.

(4) For examples of ligand-induced metal–metal bond scission in other organometallic compounds, see: (a) Lesch, D. A.; Rauchfuss, T. B. *Organometallics* **1982**, *1*, 499. (b) Richter, F.; Vahrenkamp, H. *Organometallics* **1982**, *1*, 756. (c) Johnson, B. F. G.; Lewis, J.; Nicholls, J. N.; Oxton, I. A.; Raithby, P. R.; Rosales, M. J. *J. Chem. Soc., Chem. Commun.* **1982**, 289. (d) Adams, R. D. *Polyhedron* **1985**, *4*, 2003 and references therein. (e) John, G. R.; Johnson, B. F. G.; Lewis, J.; Nelson, W. J.; McPartlin, M. J. *J. Organomet. Chem.* **1979**, *171*, C14. (f) Farrar, D. H.; Johnson, B. F. G.; Lewis, J.; Raithby, P. R.; Rosales, M. J. *J. Chem. Soc., Dalton Trans.* **1982**, 2051. (g) Goudsmi, R. J.; Johnson, B. F. G.; Lewis, J.; Raithby, P. R.; Whitmire, K. H. *J. Chem. Soc., Chem. Commun.* **1982**, 640. (h) Mercer, W. C.; Whittle, R. R.; Burkhardt, E. W.; Geoffroy, G. L. *Organometallics* **1985**, *4*, 68. (i) Mercer, W. C.; Geoffroy, G. L.; Rheingold, A. L. *Organometallics* **1985**, *4*, 1418. (j) Langenbach, H. J.; Vahrenkamp, H. *Chem. Ber.* **1979**, *112*, 3390. (k) Jackson, R. A.; Kanluen, R.; Poe, A. *Inorg. Chem.* **1984**, *23*, 523. (l) Albers, M. O.; Robinson, D. J.; Coville, N. J. *Coord. Chem. Rev.* **1986**, *69*, 127.

(5) (a) Muetterties, E. L. *Science (Washington, D.C.)* **1977**, *196*, 839. (b) Muetterties, E. L.; Rhodin, T. N.; Band, E.; Brucker, C. F.; Pretzer, W. R. *Chem. Rev.* **1979**, *79*, 91. (c) Muetterties, E. L. *J. Organomet. Chem.* **1980**, *200*, 177. (d) Muetterties, E. L. *Pure Appl. Chem.* **1982**, *54*, 83. (e) Muetterties, E. L.; Krause, M. J. *Angew. Chem., Int. Ed. Engl.* **1983**, *22*, 135.

(6) (a) Smith, A. K.; Basset, J. M. *J. Mol. Catal.* **1977**, *2*, 229. (b) Vahrenkamp, H. *Adv. Organomet. Chem.* **1983**, *22*, 169. (c) Robinson, A. L. *Science (Washington, D.C.)* **1976**, *194*, 1150. (d) Lewis, J.; Johnson, B. F. G. *Pure Appl. Chem.* **1975**, *44*, 43. (e) Pittman, C. U.; Ryan, R. C. *CHEMTECH* **1978**, 170. (f) Kaesz, H. D.; Knobler, C. B.; Andrews, M. A.; Van Buskirk, G.; Szostak, R.; Strouse, C. E.; Lin, Y. C.; Mayr, A. *Pure Appl. Chem.* **1982**, *54*, 131.

(7) See also: Deeming, A. J. In *Transition Metal Clusters*; Johnson, B. F. G., Ed.; Wiley: New York, 1980; Chapter 6.

(8) (a) Moskovits, M. *Acc. Chem. Res.* **1979**, *12*, 229. (b) Muetterties, E. L. *Bull. Soc. Chim. Belg.* **1975**, *84*, 959; **1975**, *85*, 451. (c) Kaesz, H. D. *Chem. Br.* **1973**, *9*, 344. (d) Ugo, R. *Catal. Rev.—Sci. Eng.* **1975**, *11*, 225.

(9) Richmond, M. G.; Korp, J. D.; Kochi, J. K. *J. Chem. Soc., Chem. Commun.* **1985**, 1102.

(10) (a) Pittman, C. U.; Wilemon, G. M.; Wilson, W. D.; Ryan, R. C. *Angew. Chem., Int. Ed. Engl.* **1980**, *19*, 478. (b) Ryan, R. C.; Pittman, C. U.; O'Connor, J. P. *J. Am. Chem. Soc.* **1977**, *99*, 1980. (c) Pittman, C. U.; Richmond, M. G.; Wilemon, G. M.; Absi-Halabi, M. In *Catalysis of Organic Reactions*; Kosak, J. R., Ed.; Marcel Dekker: New York, 1984; Chapter 5. (d) Wang, Y. P.; Zhang, S. M.; Wu, N.; Luo, Y. Z.; Fu, H. X. *J. Organomet. Chem.* **1986**, *307*, 65.

0020-1669/87/1326-0541$01.50/0

substitution product was isolated as black crystals in 80% yield:

$$\underset{\text{I}}{Co_4(CO)_{10}(\mu_4\text{-PPh})_2} + 4(F_2P)_2NMe \rightarrow \underset{\text{II}}{Co_4(CO)_3(\mu_4\text{-PPh})_2[(F_2P)_2NMe]_4} + 7CO \quad (1)$$

The thermal substitution of the tetracobalt cluster I was also carried out with only 1 equiv of the fluorodiphosphine ligand $(F_2P)_2NMe$. Careful examination of the reaction mixture by quantitative IR analysis indicated the same tetrakis substitution product II was formed in 25% yield, together with the unreacted precursor I. No other cobalt carbonyl species were observed.

Treatment of the tetrakis derivative II with 1 equiv of $(F_2P)_2NMe$ in toluene solution at a higher temperature of ~110 °C led to the further evolution of carbon monoxide. The pentakis derivative III could be isolated in 60–70% yield:

$$\underset{\text{II}}{Co_4(CO)_3(PPh)_2[(F_2P)_2NMe]_4} + (F_2P)_2NMe \rightarrow \underset{\text{III}}{Co_4(CO)(PPh)_2[(F_2P)_2NMe]_5} + 2CO \quad (2)$$

Slightly better yields (>90%) of III were obtained when II was treated with 5 equiv of $(F_2P)_2NMe$ at 110 °C. No other carbonyl-containing products were observed. Furthermore, when the parent cluster I was exposed to 9 equiv of $(F_2P)_2NMe$ at 110 °C, the pentakis derivative III was formed directly in 60% yield together with only traces of II.

B. Oxidative Reactions. Oxygen atom donors such as iodosylbenzene are known to be mild reagents for the oxidative decarbonylation of metal carbonyl complexes.[11] Accordingly the tetracobalt cluster I was treated with 1 equiv of iodosylbenzene in the presence of a 10-fold excess of $(F_2P)_2NMe$ in dichloromethane solution at 25 °C. Following the liberation of carbon dioxide, the analysis of the reaction mixture A by quantitative IR spectrophotometry indicated the presence of only the tetrakis derivative II in 10% yield together with the unreacted cluster I. The amounts of the tetrakis derivative II increased 2-fold (25%) when an additional 1 equiv of iodosylbenzene was added to solution A. We found no evidence of any intermediates leading to the tetrakis derivative in the resulting solution B. Finally, the addition of 6 equiv more of iodosylbenzene to solution B led to the tetrakis derivative II in 95% yield by IR analysis of solution C. When 3 equiv of iodosylbenzene was added to solution C, the pentakis derivative III was observed in ~20% yield, together with the tetrakis derivative II (~70%).

C. Reductive Reactions. Ligand substitution of the tetracobalt cluster with phosphines has been carried out efficiently by passing a cathodic current through the solution.[12] Treatment of I with 1.5 equiv of $(F_2P)_2NMe$ was similarly effected in tetrahydrofuran (THF) containing 0.3 M tetra-*n*-butylammonium perchlorate (TBAP) as the supporting electrolyte at a constant potential of −1.1 V vs. SCE. In contrast to the behavior of the other phosphines examined earlier,[12] we found that the electron-transfer chain (ETC) catalysis[13] of ligand substitution with the fluorodiphosphine $(F_2P)_2NMe$ was substantially less efficient. Thus the cathodic current was maintained until amost 1 C of charge had passed through the solution, at which point (Q = 1.05 C) the current was reversed by increasing the potential to 0 V vs. SCE. Analysis after the reoxidation of the solution (Q = 0.85 C) indicated that the monosubstituted $Co_4(CO)_8(PPh)_2[(F_2P)_2NMe]$ (IV) was formed in ~60% yield. The neutral product was isolated as a red-black solid, but repeated attempts to grow a single crystal of IV were unsuccessful.

(11) (a) Tam, W.; Lin, G. Y.; Wong, W. K.; Kiel, W. A.; Wong, V. K.; Gladysz, J. A. *J. Am. Chem. Soc.* **1982**, *104*, 141. (b) Kiel, W. A.; Buhro, W. E.; Gladysz, J. A. *Organometallics* **1984**, *3*, 879.
(12) Richmond, M. G.; Kochi, J. K. *Inorg. Chem.* **1986**, *25*, 656.
(13) For a discussion and examples of electron-transfer catalysis, see: (a) Bunnett, J. F. *Acc. Chem. Res.* **1978**, *11*, 413. (b) Saveant, J. M. *Acc. Chem. Res.* **1980**, *13*, 323. (c) Amatore, C.; Saveant, J. M.; Thiebault, A. *J. Electroanal. Chem. Interfacial Electrochem.* **1979**, *103*, 303. See also: (d) Arewgoda, M.; Robinson, B. H.; Simpson, J. *J. Am. Chem. Soc.* **1983**, *105*, 1893. (e) Chanon, M.; Tobe, M. L. *Angew. Chem., Int. Ed. Engl.* **1982**, *21*, 1.

Table I. Data Collection and Processing Parameters for $Co_4(CO)_3(PPh)_2[(F_2P)_2NMe]_4$

space group	$C2/c$, monoclinic
cell constants	
a, Å	12.184 (5)
b, Å	32.890 (11)
c, Å	11.650 (5)
β, deg	111.60 (3)
vol (V), Å^3	4340.69
mol formula	$C_{19}H_{22}Co_4F_{16}N_4O_3P_{10}$
fw	1203.86
formula units per cell (Z)	4
density (ρ), g cm^{-3}	1.84
abs coeff (μ), cm^{-1}	19.61
radiation (λ, Å)	Mo Kα (0.71073)
collection range, deg	$4 \leq 2\theta \leq 35$
scan width ($\Delta\theta$), deg	1.20 + 0.35 tan θ
max scan time, s	180
scan speed range, deg min^{-1}	0.6–5.0
total data collected	1409
indep data, $I > 3\sigma(I)$	837
total variables	160
R ($=\sum\|\|F_o\| - \|F_c\|\|/\sum\|F_o\|$)	0.090
R_w ($=[\sum w(\|F_o\| - \|F_c\|)^2/\sum w\|F_o\|^2]^{1/2}$	0.096
weights	w = 1.0

Table II. Selected Bond Distances (Å) for $Co_4(CO)_3(PPh)_2[(F_2P)_2NMe]_4$[a]

Co(1)···Co(1)′	3.444 (3)	Co(1)–P(5)	2.042 (8)
Co(1)–Co(2)	2.506 (3)	Co(2)–P(4)	2.033 (6)
Co(2)–Co(2)′	2.456 (3)	Co(2)–P(6)	1.950 (9)
Co(1)–P(1)	2.300 (4)	P(2)–N(1)	1.68 (1)
Co(1)–P(1)′	2.297 (4)	Co(1)–C(11)	2.090 (2)
Co(2)–P(1)	2.274 (4)	Co(2)–C(12)	2.012 (2)
Co(2)–P(1)′	2.364 (4)	Co(2)–C(4)	1.88 (2)
Co(1)–P(2)	2.057 (4)	P(1)–C(5)	1.81 (1)
Co(1)–P(3)	2.072 (5)	P(1)···P(1)′	2.440 (9)

[a] Numbers in parentheses represent the estimated standard deviations in the least significant digit.

The stoichiometric requirement of one electron to effect the monosubstitution of I with the fluorodiphosphine suggests that the formation of IV does not involve ETC catalysis,[13] as we recently found for the difunctional phenylphosphine $Ph_2PCH_2PPh_2$.[14] Rather, the coulometry suggests that monosubstitution of I involves only the stoichiometric reaction of the anion radical $I^{\bullet-}$ in eq 3.

$$\underset{\text{I}^{\bullet-}}{Co_4(CO)_{10}(PPh)_2^{\bullet-}} + (F_2P)_2NMe \rightarrow Co_4(CO)_8(PPh)_2[(F_2P)_2NMe]^{\bullet-} + 2CO \quad (3)$$

The latter is in accord with the requirement of a subsequent oxidation in a separate step (vide supra) to release the neutral tetracobalt cluster, i.e.

$$Co_4(CO)_8(PPh)_2[(F_2P)_2NMe]^{\bullet-} \xrightarrow{-e^-} \underset{\text{IV}}{Co_4(CO)_8(PPh)_2[(F_2P)_2NMe]} \quad (4)$$

The electrochemical studies to be described in a later section (Table IV) verify this conclusion.[15]

II. Molecular Structures of the Fluorodiphosphine-Substituted Tetracobalt Clusters. Although a single crystal of the tetrakis derivative II was successfully grown from hexane at −20 °C, repeated attempts to grow single crystals suitable for the X-ray

(14) Richmond, M. G.; Kochi, J. K. *Organometallics*, in press.
(15) The substitution of $Co_4(CO)_{10}(PPh)_2$ with P = phosphines and phosphites leads to derivatives that are more difficult to reduce. Thus, the driving force for the electron-transfer step in ETC catalysis is exergonic. On the other hand, fluorophosphine substitution stabilizes the anion radical by shifting the reduction potential to more positive values. Accordingly the driving force for electron transfer with fluorophosphine derivatives either is thermoneutral or is not as exergonic. The latter tends toward a substitution process which is (electron) stoichiometric.

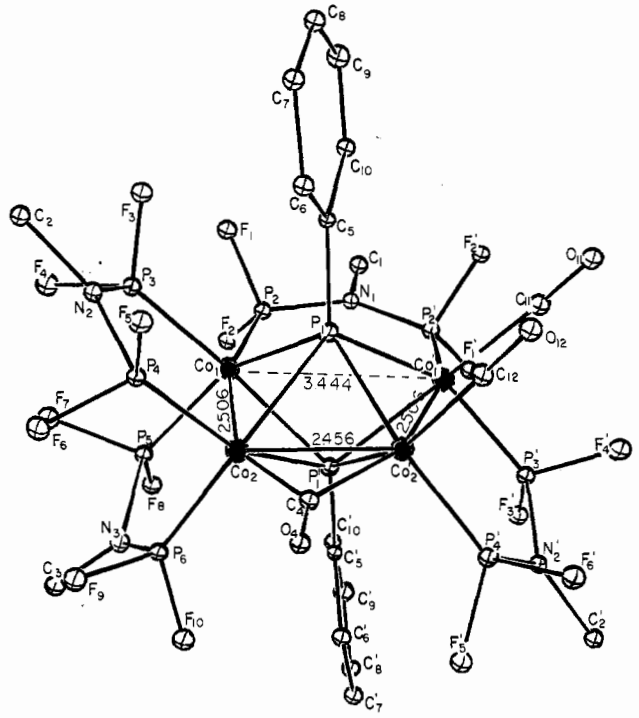

Figure 1. ORTEP diagram of $Co_4(CO)_3(PPh)_2[(F_2P)_2NMe]_4$ with numbering scheme showing the two distinct types of bidentate $(F_2P)_2NMe$ ligands. The hydrogen atoms are omitted for clarity.

crystallography of the respective mono and the pentakis derivatives IV and III failed. Nonetheless, the combination of the X-ray determination of II together with the ^{31}P NMR and IR spectral assignments allowed us to deduce the structures of the mono and pentakis derivatives.

A. The X-ray crystallographic data and processing parameters for the tetrakis derivative II are given in Table I. A 50% disorder exists between one of the fluorodiphosphines and the two carbonyls related by a 2-fold axis that remains even when the refinement is done in space group *Cc*. This accounts for the poor scattering of the crystal and the somewhat high *R* value.

The molecular structure of the tetrakis derivative II is shown in Figure 1 together with the numbering scheme for the principal atoms. The structure in Figure 1 shows the presence of only three intact Co–Co bonds. The large separation of 3.444 (3) Å between Co(1) and Co(1)′ (shown in Figure 1 and Table II) precludes any direct bonding interaction between these cobalt centers.[16] The noncarbonyl-bridged Co(1)–Co(2) distance 2.506 (3) Å is 0.19 Å shorter than the corresponding bonds in the parent tetracobalt cluster I.[17] Moreover, the lone carbonyl-bridged Co(2)–Co(2)′ distance of 2.456 (3) Å is 0.06 Å shorter than those observed in I. These bond lengths are the shortest metal–metal distances reported to date in the growing family of phosphinidene-capped tetracobalt clusters.[17,18]

The bonds to the capping phosphinidene are also affected by fluorodiphosphine substitution. For example, the Co–μ_4-P distances vary from 2.274 to 2,364 Å (with an average of 2.309 Å), which compares with the reported distance of 2.245 Å (average) in $Co_4(CO)_{10}(PPh)_2$.[17] The μ_4-P–μ_4-P nonbonded distance of 2.440 Å is the shortest known phosphinidene distance, being ~0.01 Å shorter than that in $Co_4(CO)_{10}(PPh)_2$ and only 0.2 Å longer than that generally accepted for the P–P single bond.[19] Such a contraction of the intercap distance clearly results from the cleft in the cluster as a result of the scission of the Co(1)–Co(1)′ bond in I and the concomitant widening of the bond angle Co(1)–μ_4-P–Co(1)′ from 69° in I to 97° in II (see Table III).[20] On the other hand, the bonds to the ligands (i.e., Co–PF_2) are relatively unchanged—ranging from 1.950 to 2.072 Å with a mean distance of 2.031 Å, which are in agreement with those reported in various cobalt phosphines.[21]

Finally, both phenyl groups on the phosphinidene caps are canted toward the cleft in the Co_4 core by 7°, as illustrated in Figure 2. By way of comparison, both phenyl groups are collinear with the nonbonded μ_4-P···μ_4-P axis in the parent tetracobalt cluster I possessing idealized D_{2h} symmetry.

B. The $^{31}P\{^1H\}$ NMR spectrum of the tetrakis derivative II in chloroform-d_1 solution at 25 °C consists of a broad resonance at δ 160 and a high-field resonance at δ −69 in a 4:1 integral ratio. We assign the low-field unresolved multiplet at δ 160 to overlapping resonances arising from the pair of μ_4-phosphinidene caps and three $(F_2P)_2NMe$ ligands that bridge the Co(1)–Co(2) and Co(2)′–Co(1)′ bonds[22,23] (see Figure 1). (Note that the μ_4-phosphinidene chemical shift at δ 135 in the parent cluster $Co_4(CO)_{10}(PPh)_2$ is sensitive to substitution, particularly of phosphorus(III) ligands.[14]) The unique $(F_2P)_2NMe$ that bridges the cleft in the cluster between Co(1) and Co(1)′ is responsible for the high-field resonance at δ −69.[24-27] Moreover, the carbonyl has also been observed in other systems.[25]

Table III. Selected Bond Angles (deg) for $Co_4(CO)_8(PPh)_2[(F_2P)_2NMe]_4$[a]

Co(1)–Co(2)–Co(2)′	101.26 (5)	Co(1)–P(1)–Co(1)′	97.0 (2)
Co(1)–P(1)–Co(2)	66.4 (1)	Co(2)–P(1)–Co(2)′	63.9 (1)
Co(1)–P(1)–Co(2)′	110.7 (2)		
P(1)–Co(1)–P(1)′	64.1 (2)	Co(2)–C(4)–Co(2)′	81.3 (7)
P(1)–Co(2)–P(1)′	63.5 (2)	Co(1)–P(1)–C(5)	119.0 (10)
Co(1)–P(2)–N(1)	128.7 (2)	Co(1)′–P(1)–C(5)	118.0 (10)
Co(1)–P(3)–N(2)	119.8 (3)	Co(2)–P(1)–C(5)	126.0 (10)
Co(1)–P(5)–N(3)	115.4 (5)	Co(2)′–P(1)–C(5)	128.0 (10)

[a] Numbers in parentheses are estimated standard deviations in the least significant digit.

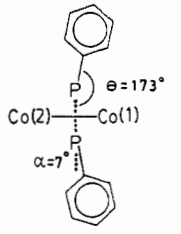

Figure 2. Side view (from the cleft) of $Co_4(CO)_3(PPh)_2[(F_2P)_2NMe]_4$ showing the tilt of the phenylphosphinidene moiety from the normal plane.

(16) Pauling, L. *Nature of the Chemical Bond*, 3rd ed.; Cornell University Press: Ithaca, NY, 1960.
(17) (a) Ryan, R. C.; Dahl, L. F. *J. Am. Chem. Soc.* **1975**, *97*, 6904. (b) Ryan, R. C.; Pittman, C. U., Jr.; O'Connor, J. P.; Dahl, L. F. *J. Organomet. Chem.* **1980**, *193*, 247.
(18) (a) Richmond, M. G.; Kochi, J. K. *Inorg. Chem.* **1986**, *25*, 1334. (b) Richmond, M. G.; Kochi, K. *Organometallics*, in press. (c) See also ref 14.
(19) Corbridge, D. E. C. *Top. Phosphorus Chem.* **1966**, *3*, 57.
(20) The internal Co(1)–Co(2)–Co(2)′ bond angle is also widened from 89° in I to 101° in II (see Table III).
(21) (a) Newton, M. G.; King, R. B.; Chang, M.; Pantaleo, N. S.; Gimeno, J. *J. Chem. Soc., Chem. Commun.* **1977**, 531. (b) Newton, M. G.; Pantaleo, N. S.; King, R. B.; Lotz, T. J. *J. Chem. Soc., Chem. Commun.* **1978**, 514. (c) King, R. B.; Chang, M.; Newton, M. G. *J. Organomet. Chem.* **1985**, *296*, 15.
(22) The ^{31}P resonance(s) associated with the μ_4-phosphinidene capping ligands in other clusters of this type are found to be considerably broadened due to coupling with the quadrupolar ^{59}Co ($I = {}^7/_2$) nuclei.
(23) The ^{31}P resonances assigned to the fluorophosphine ligands appear broadened possibly due to the coupling of the quadrupolar ^{59}Co and ^{14}N ($I = 1$) nuclei.
(24) Such a high-field resonance in the ^{31}P NMR spectra, which is indicative of fluorophosphine ligation of cobalt centers possessing no formal bonding interactions, i.e.

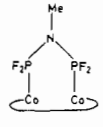

groups in II are identified in the IR spectrum by a pair of bands at 2021 and 1988 cm^{-1} for the terminal CO's and a band at 1817 cm^{-1} for the single bridging CO. By comparison, the pentakis derivative III shows only one band at 1811 cm^{-1} in the carbonyl region of the IR spectrum, which is diagnostic of a single bridging CO. This simple IR spectrum, coupled with a $^{31}P\{^1H\}$ NMR spectrum which is similar to that of III (viz., a broad low-field resonance at δ 160 and a high-field singlet at δ −54) but with a 5:1 integral ratio, readily leads to the structure of the pentakis derivative as[28]

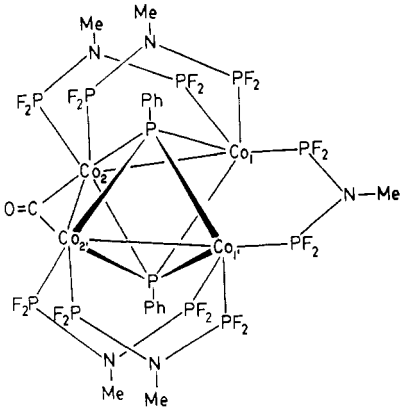

III

Similarly, the structure of the mono derivative IV can be deduced from its IR and NMR spectra. Thus, the $^{31}P\{^1H\}$ NMR spectrum of $Co_4(CO)_8(PPh)_2[(F_2P)_2NMe]$ (IV) in chloroform-d_1 showed only a single broad resonance at δ 160. The partial resolution of this resonance as a triplet (from P–F splittings)[29] suggests that both phosphorus atoms in the bound $(F_2P)_2NMe$ are equivalent. This together with the presence of only a single band at 1881 cm^{-1} in the IR spectrum (for a bridging carbonyl group) supports a symmetrical structure such as

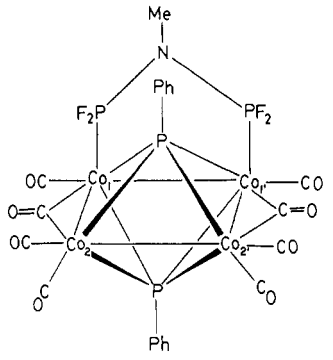

IV

(25) (a) Carty, A. J. *Pure Appl. Chem.* **1982**, *54*, 113. (b) Carty, A. J. *Adv. Chem. Ser.* **1982**, *No. 196*, 163. (c) Garrou, P. E. *Chem. Rev.* **1981**, *81*, 186. (d) Carty, A. J.; Maclaughlin, S. A.; Taylor, N. J. *J. Organomet. Chem.* **1981**, *204*, C27. (e) Wojcicki, A.; Shyu, S. G. *Organometallics* **1985**, *4*, 1457. (f) Kreter, P. E.; Meek, D. W. *Inorg. Chem.* **1983**, *22*, 319. (g) Geoffroy, G. L.; Rosenberg, S.; Shulman, P. M.; Whittle, R. R. *J. Am. Chem. Soc.* **1984**, *106*, 1519. (h) Rosenberg, S.; Whittle, R. R.; Geoffroy, G. L. *J. Am. Chem. Soc.* **1984**, *106*, 5934. (i) Cf. ref 27.

(26) For the only other known examples of $(F_2P)_2NMe$ ligating two metals not joined by a metal–metal bond, see: (a) Newton, M. G.; King, R. B.; Chang, M.; Gimeno, J. *J. Am. Chem. Soc.* **1977**, *99*, 2802. (b) Newton, M. G.; King, R. B.; Chang, M.; Gimeno, J. *J. Am. Chem. Soc.* **1978**, *100*, 1632.

(27) There are exceptions to this generalization. For example, see: (a) Targos, T. S.; Geoffroy, G. L.; Rheingold, A. L. *J. Organomet. Chem.* **1986**, *299*, 223. (b) Gelmini, L.; Matassa, L. C.; Stephan, D. W. *Inorg. Chem.* **1985**, *24*, 2585. (c) Rosen, R. P.; Hoke, J. B.; Whittle, R. R.; Geoffroy, G. L.; Hutchinson, J. P.; Zubieta, J. A. *Organometallics* **1984**, *3*, 846.

(28) Additional support for this structure of the pentakis derivative is provided by correlation spectra by multiple resonance techniques of the ^{31}P and ^{19}F NMR resonances (unpublished results).

(29) With a splitting of ~1100 Hz.

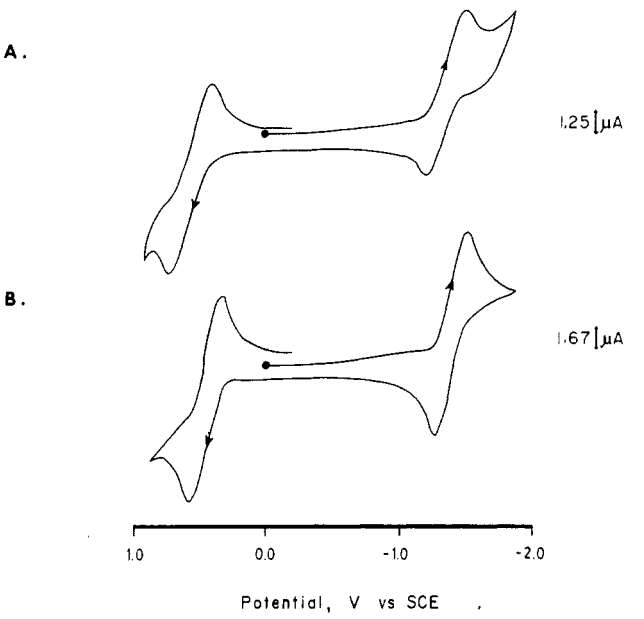

Figure 3. Initial negative-scan cyclic voltammograms of (A) $Co_4(CO)_3(PPh)_2[(F_2P)_2NMe]_4$ and (B) $Co_4(CO)(PPh)_2[(F_2P)_2NMe]_5$ in THF containing 0.3 M TBAP at 500 mV s^{-1} and 298 K.

Indeed such symmetrically bridged structures have been recently elucidated by the X-ray crystallography of the related difunctional phenylphosphine derivative $Co_4(CO)_8(PPh)_2[(Ph_2P)_2CH_2]$.[14] The similarity of the IR spectrum of this derivative in the carbonyl region with that of IV is consistent with the structure proposed above.

III. Oxidation–Reduction of Fluorophosphine-Substituted Tetracobalt Clusters. The redox behavior of the tetrakis and pentakis derivatives II and III was examined by cyclic voltammetry at a platinum electrode in THF solutions containing 0.3 M TBAP. Figure 3A shows the cyclic voltammogram (CV) of $Co_4(CO)_3(PPh)_2[(F_2P)_2NMe]_4$ to consist of two well-defined redox couples at $E_{1/2}$ = −1.31 and +0.58 V vs. SCE at a scan rate of 500 mV s^{-1}. The first CV wave A is chemically reversible as shown by the ratio i_p^c/i_p^a of the cathodic and anodic peak currents of close to unity and the current function, which varies linearly with the square root of the scan rate v (not shown).[30,31] Calibration of the peak current with that of a ferrocene standard[32] and bulk coulometric measurements establish the reversible CV wave at $E_{1/2}$ = −1.31 V to represent the one-electron 0/−1 redox couple; i.e.

$$\text{II} \xrightarrow{+e^-} \text{II}^{\bullet -}$$

The second CV wave with $E_{1/2}$ = +0.58 V is also reversible, as judged by the electrochemical criteria described above. Furthermore, the calibration of the peak current with ferrocene, as well as bulk coulometric measurements, establishes this CV wave to represent the one-electron 0/+1 redox couple, i.e.

$$\text{II} \xrightarrow{-e^-} \text{II}^{\bullet +}$$

The cyclic voltammogram of the pentakis derivative $Co_4(CO)(PPh)_2[(F_2P)_2NMe]_5$ (III) shown in Figure 3B also consists of two well-defined one-electron redox couples. The reversible CV waves $E_{1/2}$ = −1.36 and +0.49 V vs. SCE represent the 0/−1

(30) Bard, A. J.; Faulkner, L. R. *Electrochemical Methods*; Wiley: New York, 1980.

(31) Note that the separation of ~300 mV of the cathodic and anodic peak potentials indicate that the CV is not electrochemically reversible to this sweep rate.

(32) (a) Gagne, R. R.; Koval, C. A.; Lisensky, G. C. *Inorg. Chem.* **1980**, *19*, 2854. (b) Koepp, H. M.; Wendt, H.; Stehlow, H. *Z. Z. Elektrochem.* **1960**, *64*, 483.

(33) Howell, J. O.; Goncalves, J. M.; Amatore, C.; Klasinc, L.; Wightman, R. M.; Kochi, J. K. *J. Am. Chem. Soc.* **1984**, *106*, 3968.

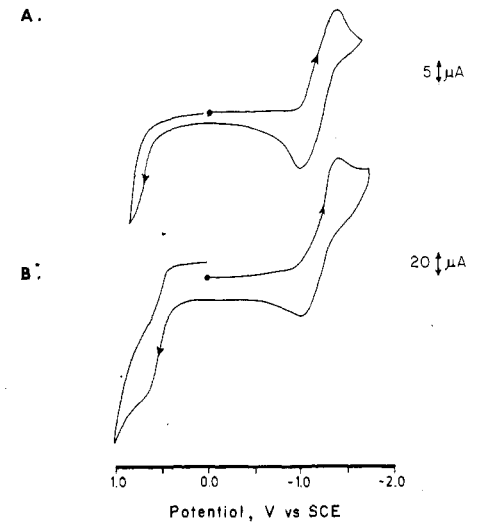

Figure 4. Initial negative-scan cyclic voltammograms of (A) $Co_4(CO)_{10}(PPh)_2$ and (B) $Co_4(CO)_8(PPh)_2[(F_2P)_2NMe]$ in THF containing 0.3 M TBAP at 500 mV s^{-1} and 298 K.

Table IV. Cyclic Voltammetry of Tetracobalt Clusters[a]

	redn[b]			oxidn		
Co_4 cluster	E_p^c	E_p^a	$E_{1/2}$	E_p^a	E_p^c	$E_{1/2}$
I	−1.41	−1.02	−1.22			
IV	−1.42	−1.09	−1.25	+0.70		
II	−1.46	−1.17	−1.31	+0.73	+0.43	+0.58
III	−1.49	−1.23	−1.36	+0.62	+0.36	+0.49

[a] In $\sim 10^{-3}$ M THF solutions containing 0.3 M TBAP at a scan rate of 500 mV s^{-1}. Potentials are in volts relative to SCE, calibrated with ferrocene. [b] E_p^c and E_p^a refer to the cathodic and anodic peak potentials of the CV waves. When both (coupled) waves are observed, the chemically reversible redox couple is approximated by the half-wave potential $E_{1/2} = (E_p^c + E_p^a)/2$.[33]

and 0/+1 redox couples analogous to those for the tetrakis derivative.

The electrochemical production of the anion radicals $II^{\bullet-}$ and $III^{\bullet-}$ of the tetrakis and pentakis derivatives was indicated by the clean uptake of one electron during bulk electrolysis. In both cases however, the red-black solutions were EPR silent. Attempts to isolate the salts as single crystals suitable for X-ray crystallography were unsuccessful. Similarly the production of the cation radicals $II^{\bullet+}$ and $III^{\bullet+}$ of the tetrakis and pentakis derivatives was clearly indicated by the coulometry during bulk oxidation. Attempts to isolate crystalline salts from the dark red solutions were unsuccessful.

The cyclic voltammogram of the mono derivative $Co_4(CO)_8(PPh)_2[(F_2P)_2NMe]$ (IV) is shown in Figure 4, together with that obtained from the parent cluster I. The gross features of both cyclic voltammograms are similar to those obtained in Figure 3 from the tetrakis and pentakis derivatives II and III—with two exceptions. First, at the same sweep rate of 500 mV s^{-1}, the redox couple 0/−1 of IV at $E_{1/2} \simeq -1.22$ V vs. SCE is chemically less reversible than that of either II or III. Second, the redox couple 0/+1 of IV at $E_p^a \approx +0.7$ V is irreversible under conditions where it is reversible in II and III. We thus conclude that both the anion radical and the cation radicals of the tetracobalt cluster I as well as ion radicals of the mono(fluorodiphosphine) derivative IV are all less stable than those of the poly(fluorodiphosphine) analogues. The redox potentials are summarized in Table IV.

Discussion

The interaction of the tetracobalt cluster $Co_4(CO)_{10}(PPh)_2$ (I) thermally with the difunctional fluorophosphine $(F_2P)_2NMe$ is unique in two important ways.

First, the structure of the multiply substituted tetracarbonyl cluster II is unusual. Thus, the X-ray diffraction analysis reveals two types of binding of the fluorodiphosphine ligand to the tetracobalt cluster. Three of the $(F_2P)_2NMe$ ligands bridge two cobalt centers across the Co(1)–Co(2) bond to form overall a conventional five-membered ring (see Figure 1). The unique fourth $(F_2P)_2NMe$ is observed to ligate two cobalt atoms (Co(1) and Co(1)′) which are not bonded directly. Such a ligation of a pair of nonbonded metals by $(F_2P)_2NMe$ has been observed in the iron dimer $Fe_2(CO)_6[(F_2P)_2NMe]_2$—but it readily suffered CO loss, followed by the formation of the Fe–Fe bond to afford $Fe_2(CO)_5[(F_2P)_2NMe]$.[26a,34] Interestingly, the latter process is not observed in the tetracobalt cluster to regenerate the fourth Co–Co bond and return the cluster polyhedron to its initially closed configuration. Moreover, such a transformation is also not observed when the last two terminal CO groups are replaced in II by a fifth fluorodiphosphine ligand (see eq 2).

Second, the multiple replacement of seven carbonyl ligands to afford the tetrakis derivative II is unusual in that it occurs without any evidence of intermediates. Even the employment of mild reaction conditions (with iodosylbenzene as an effective decarbonylating agent for I) gives no indication of tetracobalt intermediates that contain fewer than four fluorodiphosphine ligands. It is extremely likely however that the complex transformation in eq 1 does proceed in a stepwise manner.[36] If so, the initial substitution with a single fluorodiphosphine ligand

$$Co_4(CO)_{10}(PPh)_2 + (F_2P)_2NMe \rightarrow Co_4(CO)_8(PPh)_2[(F_2P)_2NMe] + 2CO \quad (5)$$

must be followed in rapid succession by a second, a third, and finally a fourth fluorodiphosphine ligand. The separate treatment of the tetrakis derivative II with fluorodiphosphine in eq 2 shows that the replacement of the last two CO's to afford the pentakis derivative III is relatively slow. Such a facile multiple ligand substitution has also been observed with the triruthenium cluster $Ru_3(CO)_{12}$, which yielded the tris-substitution product $Ru_3(CO)_9P_3$ directly upon treatment with phosphines (P).[37,38] No intermediates were observed.

Our inability to observe any intermediate precludes the establishment of the point at which metal–metal bond scission occurs in the substitution sequence. Although the electron-induced substitution of the tetracobalt cluster in eq 3 and 4 produces the monosubstitution product IV, its structure is not necessarily pertinent to that generated thermally in the first stage (see eq 5).[39] In order to probe this question, let us consider the effect of fluorodiphosphine ligands on the tetracobalt cluster.

Thus, the difunctional fluorophosphine $(F_2P)_2NMe$ differs from its phenyldiphosphine analogues $(Ph_2P)_2CH_2$ (dppm), $(Ph_2P)_2(CH_2)_2$ (dppe), and $(Ph_2P)_2(CH)_2$ (dppt), which we found to interact with the tetracobalt only as bridging ligands between Co–Co bonds.[14] Indeed, these last three ligands do not encourage extensive electron delocalization to the cluster framework owing to their saturated nature. On the other hand, in $(F_2P)_2NMe$ the $p\pi$–$d\pi$ orbital interactions between the nitrogen and phosphorus centers, which are enhanced by the electronegative fluorines,

(34) Bridging of nonbonded iron atoms has also been observed in the triiron cluster $Fe_3(CO)_7(PPh)_2(Ph_2PCH_2CH_2PPh_2)$, which is formed circuitously by a stereomutation of the cluster polyhedron.[35]
(35) Ohst, H. H.; Kochi, J. K. *Inorg. Chem.* **1986**, *25*, 2066.
(36) For the phosphorus(III)-induced acceleration in substitution reactions involving other metal clusters, see: (a) Karel, K. J.; Norton, J. R. *J. Am. Chem. Soc.* **1974**, *96*, 6812. (b) Darensbourg, D. J.; Baldwin-Zuschke, B. J. *J. Am. Chem. Soc.* **1982**, *104*, 3906. (c) Sonnenberger, D. C.; Atwood, J. D. *Organometallics* **1982**, *1*, 694. (d) Poe, A.; Sekhar, V. C. *Inorg. Chem.* **1985**, *24*, 4376. (e) Sonnenberger, D. C.; Atwood, J. D. *J. Am. Chem. Soc.* **1982**, *104*, 2113. (f) Atwood, J. D.; Wovkulich, M. J.; Sonnenberger, D. C. *Acc. Chem. Res.* **1983**, *16*, 350.
(37) Candlin, J. P.; Shortland, A. C. *J. Organomet. Chem.* **1969**, *16*, 289.
(38) Ligand substitution in $Ru_3(CO)_{12-n}P_n$ (n = 1, 2) clusters shows greater proclivity toward CO dissociation than $Ru_3(CO)_{12}$, Cf: (a) Poe, A. J.; Twigg, M. V. *J. Organomet. Chem.* **1973**, *50*, C39. (b) Poe, A. J.; Twigg, M. V. *J. Chem. Soc., Dalton Trans.* **1974**, 1860. (c) Keeton, D. P.; Malik, S. K.; Poe, A. *J. Chem. Soc., Dalton Trans.* **1977**, 233. (d) Malik, S. K.; Poe, A. *Inorg. Chem.* **1978**, *17*, 1484. (e) Malik, S. K.; Poe, A. *Inorg. Chem.* **1979**, *18*, 1241. (f) See also ref 36.
(39) Thus, substitution under thermal conditions presumably occurs on the neutral tetracobalt cluster, whereas it undoubtedly occurs on the anion radical under reductive conditions.

promote a delocalized ligand-cluster system.[40] In this sense the fluorodiphosphine is more akin to a phosphinidene or a phosphide group than a diphosphine or phosphite. This qualitative conclusion is indeed supported by the redox behavior shown in Figures 3 and 4. Thus, the perturbation of the tetracobalt cluster by the replacement of a pair of carbonyls by a single fluorodiphosphine ligand (as in IV) is significantly less than that by the difunctional phenylphosphines *dppm*, *dppe* or *dppt*.[41] However, the presence of four or five $(F_2P)_2NMe$ ligands as in II and III leads to stable anion radicals as well as cation radicals of the tetracobalt cluster (vide supra). Thus, the fluorodiphosphine ligand can be considered to be amphoteric in its ability to delocalize electron density, which is either accepted from or donated to the cluster via low-lying π and π^* orbitals.[42,43] In this regard the fluorodiphosphine ligand may be considered to be an "electron reservoir".[43,44] If such fluorodiphosphine–cobalt interactions are important, it seems reasonable that the ligand-induced scission of the Co–Co bond will occur at that juncture involving the maximum practical number of $(F_2P)_2NMe$ attachments. The latter points to the last (fourth) substitution step, in which each nonbonded Co(1)–Co(1)′ center can best accommodate an 18-electron count. This situation apparently persists in the pentakis derivative despite the steric overcrowding induced by the presence of the fifth $(F_2P)_2NMe$.

The scission of the polyhedral cluster framework observed upon ligand substitution may be considered within the context of the Wade–Mingos rules.[45] This working theory indicates that an *n*-vertex closo polyhedron will normally have $n + 1$ bonding molecular orbitals associated with the skeleton. For the six-vertex clusters of the *closo*-M_4E_2 type, of which $Co_4(CO)_{10}(PPh)_2$ is a member, the critical number of skeletal electron pairs can be 8 for the theoretical reasons elaborated by Halet, Hoffmann, and Saillard.[46,47] Thus, the addition of one two-electron-donor ligand to the Co_4P_2 framework is expected to afford a six-vertex nido cluster possessing nine electron pairs. In both the tetrakis and pentakis derivatives II and III, the number of ancillary two-electron donor ligands is 11, which is one more than found in the parent $Co_4(CO)_{10}(PPh)_2$, and the coordination of the extra donor ligand provides the extra skeletal electron pair necessary for the polyhedral expansion, as observed. (The resulting product may be viewed as a cluster derived by removal of an equatorial vertex from a closo pentagonal bipyramid.)

Experimental Section

Materials. Bis(difluorophosphino)methylamine was prepared according to the procedure of Nixon.[48] The tetracobalt cluster $Co_4(CO)_{10}(PPh)_2$ was synthesized from sodium tetracarbonylcobaltate and dichlorophenylphosphine.[12] Iodosylbenzene was prepared from iodosylbenzene diacetate (Aldrich).[49] Toluene, benzene, hexane, and THF were distilled from sodium benzophenone and stored under argon. Tetra-*n*-butylammonium perchlorate (G. F. Smith Chemical) was recrystallized twice from a mixture of hexane and ethyl acetate and dried in vacuo prior to use.

Synthesis of $Co_4(CO)_3(PPh)_2[(F_2P)_2NMe]_4$. To 0.5 g (0.68 mmol) of $Co_4(CO)_{10}(PPh)_2$ in a Fischer–Porter tube was added 10 mL of benzene, followed by 0.9 mL (~5.4 mmol) of $(F_2P)_2NMe$. The vessel was sealed and heated overnight at 60 °C. After it was cooled, the reaction mixture was concentrated in vacuo to afford a black residue. Purification by chromatography on silica gel with benzene furnished the product cluster $Co_4(CO)_3(PPh)_2[(F_2P)_2NMe]_4$. An analytically pure sample and crystals suitable for X-ray diffraction analysis were obtained by recrystallization from hexane at −20 °C to yield 0.65 g (79% yield) of black $Co_4(CO)_3(PPh)_2[(F_2P)_2NMe]_4$. IR($CH_2Cl_2$; ν_{CO}, cm^{-1}): 2021.3 (vs), 1988.1 (m), 1817.2 (m). UV (CH_2Cl_2; λ_{max}, nm (ϵ)): 572 (2185), 488 (5254), 328 (10784), 283 (16970). ^1H NMR ($CDCl_3$, 25 °C): δ 1.85 (9 H, b s), 3.10 (3 H, b s), 6.96 (6 H, b), 7.82 (4 H, b). $^{31}P\{^1H\}$ NMR ($CDCl_3$, 25 °C): δ 162.0 (b t, J_{P-F} = 1160 Hz), −68.8 (b t, J_{P-F} = 561 Hz). Anal. Calcd for $C_{19}H_{22}Co_4F_{16}N_4P_{10}O_3$: C, 18.94; H, 1.83; N, 4.65. Found: C, 19.07; H, 1.88; N, 4.55.

Interaction of $Co_4(CO)_{10}(PPh)_2$ and $(F_2P)_2NMe$ in the Presence of Iodosylbenzene. To 0.2 g (0.27 mmol) of $Co_4(CO)_{10}(PPh)_2$ and 0.6 mL (~3.6 mmol) of $(F_2P)_2NMe$ in 25 mL of CH_2Cl_2 was added 0.06 g (0.27 mmol) of iodosylbenzene. The reaction was stirred overnight at room temperature and then examined by IR spectroscopy to reveal the presence of $Co_4(CO)_3(PPh)_2[(F_2P)_2NMe]_4$ (~10%), in addition to unreacted starting cluster (~90%). No evidence for any intermediates leading to the tetrasubstituted cluster was observed. The identity of the tetrasubstituted cluster was readily ascertained by its bridging carbonyl band at 1823 cm^{-1} in the IR spectrum. At this point, an additional 2.0 equiv (0.55 mmol) of iodosylbenzene was added to the reaction mixture. After the solution was stirred for 6.0 h, the IR analysis of an aliquot revealed an additional conversion to $Co_4(CO)_3(PPh)_2[(F_2P)_2NMe]_4$ (~25%). The reaction was next treated with more iodosylbenzene (6.3 equiv, 1.70 mmol) and monitored by IR analysis after gas evolution (CO_2) had ceased (~5–10 min). The IR spectrum showed essentially complete conversion to $Co_4(CO)_3(PPh)_2[(F_2P)_2NMe]_4$ at this juncture (~95%). Again no evidence for any intermediates leading to $Co_4(CO)_3(PPh)_2[(F_2P)_2NMe]_4$ was observed at any point during these decarbonylation reactions. Final treatment of the reaction solution with an additional 3.4 equiv (0.91 mmol) of iodosylbenzene slowly afforded the pentasubstituted cluster $Co_4(CO)(PPh)_2[(F_2P)_2NMe]_5$, as evidenced by a decrease in the terminal carbonyl bands of $Co_4(CO)_3(PPh)_2[(F_2P)_2NMe]_4$ and a slight shift of the bridging carbonyl band to ~1815 cm^{-1}, consistent with the IR spectrum of $Co_4(CO)(PPh)_2[(F_2P)_2NMe]_5$.

Synthesis of $Co_4(CO)(PPh)_2[(F_2P)_2NMe]_5$. To 0.5 g (0.68 mmol) of $Co_4(CO)_{10}(PPh)_2$ in a Fischer–Porter tube was added 20 mL of toluene and 1.0 mL (~6.0 mmol) of $(F_2P)_2NMe$. The reaction vessel was sealed and heated at ~110 °C for 6.0 h and then allowed to cool. TLC examination with a 7:3 v/v mixture of benzene and hexane indicated essentially quantitative conversion to a slower moving material. The reaction mixture was concentrated in vacuo, and the resulting black residue was then purified by chromatography over silica gel using the above solvent system. An analytically pure sample was recrystallized from hexane at −40 °C to afford 0.55 g (62% yield) of black $Co_4(CO)(PPh)_2[(F_2P)_2NMe]_5$. IR ($CH_2Cl_2$; ν_{CO}, cm^{-1}): 1811.3 (m). UV (CH_2Cl_2; λ_{max}, nm(ϵ)): 572 (2689), 450 (7189), 330 (14608), 285 (23556). ^1H NMR ($CDCl_3$, 25 °C): δ 1.87 (12 H, b s), 3.15 (3 H, b s), 6.92 (6 H, b), 7.88 (4 H, b). $^{31}P\{^1H\}$ NMR ($CDCl_3$, 25 °C): δ 159.6 (b t, J_{P-F} = 1020 Hz), −54.1 (b s). Anal. Calcd for $C_{18}H_{25}Co_4F_{20}N_5P_{12}O$: C, 16.43; H, 1.90; N, 5.32. Found: C, 16.48; H, 1.94: N, 5.31.

Instrumentation. Infrared spectra were recorded on a Nicolet 10DX FT spectrometer in either 0.1- or 1.0-mm NaCl cells. The UV–vis spectra were recorded on a Hewlett--Packard 8450A diode array spectrometer. The ^{31}P (36.2 MHz) and ^1H (89.6 MHz) NMR spectra were recorded on a JEOL FX-90Q spectrometer. The ^{31}P and ^1H NMR data are referenced to external 85% H_3PO_4 and tetramethylsilane, respectively. Positive chemical shifts are to low field of the external standard.

Electrochemical Measurements. Cyclic voltammetry was performed at a platinum electrode with an *iR*-compensated potentiostat[50] driven by

(40) For examples of lowered nitrogen basicity in similar systems due to $p\pi$–$d\pi$ interaction, see: (a) Cowley, A. H.; Hnoosh, M. H. *J. Am. Chem. Soc.* **1966**, *88*, 2595. (b) Cowley, A. H.; Pinnell, R. P. *J. Am. Chem. Soc.* **1965**, *87*, 4454. (c) Hedberg, E.; Hedberg, L.; Hedberg, K. *J. Am. Chem. Soc.* **1974**, *96*, 4417. (d) Romming, C.; Songstad, J. *Acta Chem. Scand., Ser. A* **1978**, *A32*, 689. (e) Cotton, F. A.; Riess, J. G.; Stults, B. R. *Inorg. Chem.* **1983**, *22*, 133. (f) Hart, W. A.; Sisler, H. H. *Inorg. Chem.* **1964**, *3*, 617.

(41) Thus these σ-donor ligands with less accessible π^* orbitals tend to destabilize the 0/−1 redox couple while stabilizing the 0/+1 redox couple.[14]

(42) For discussion and examples of donor/acceptor properties of ligands, see: (a) Cotton, F. A.; Wilkinson, G. *Advanced Inorganic Chemistry: A Comprehensive Text*; Wiley: New York, 1980. (b) Dobson, G. R.; Stolz, I. W.; Sheline, R. K. *Adv. Inorg. Chem. Radiochem.* **1966**, *8*, 1.

(43) King, R. B. *Acc. Chem. Res.* **1980**, *13*, 243.

(44) (a) Lauher, J. W. *J. Am. Chem. Soc.* **1978**, *100*, 5305; **1979**, *101*, 2604. (b) Penfold, B. R.; Robinson, B. H. *Acc. Chem. Res.* **1973**, *6*, 73.

(45) (a) Wade, K. *Adv. Inorg. Chem. Radiochem.* **1976**, *18*, 1. (b) Wade, K. In *Transition Metal Clusters*; Johnson, B. F. G., Ed.; Wiley: New York, 1980; Chapter 3. (c) Johnson, B. F. G.; Benfield, R. E. *Top. Stereochem.* **1981**, *12*, 253. (d) Mingos, D. M. P. *Nature (London), Phys. Sci.* **1972**, *236*, 99. (e) Grimes, R. N. *Acc. Chem. Res.* **1978**, *11*, 420. (f) Wade, K. *Chem. Br.* **1975**, *11*, 177.

(46) Halet, J. F.; Hoffmann, R.; Saillard, J. Y. *Inorg. Chem.* **1985**, *24*, 1695. Compare also: Ohst, H. H.; Kochi, J. K. *Organometallics* **1986**, *5*, 1359.

(47) The associate editor has pointed out that complexes I–IV also fit within the TEC rules of Teo. See: Teo, B. K. *Inorg. Chem.* **1984**, *23*, 1251. Teo, B. K.; Longoni, G.; Chung, F. R. K. *Inorg. Chem.* **1984**, *23*, 1257.

(48) Nixon, J. F. *J. Chem. Soc. A* **1968**, 2689.

(49) Saltzman, H.; Sharefkin, J. G. *Organic Synthesis*; Wiley: New York, 1973; Collect. Vol. V, p 658.

(50) (a) Garreau, D.; Saveant, J. M. *J. Electroanal. Chem. Interfacial Electrochem.* **1972**, *35*, 309. (b) Garreau, D.; Saveant, J. M. *J. Electroanal. Chem. Interfacial Electrochem.* **1974**, *50*, 22.

Table V. Final Positional Parameters for the Non-Hydrogen Atoms of $Co_4(CO)_3(PPh)_2[(F_2P)_2NMe]_4$[a]

atom	x	y	z	B, Å²	atom	x	y	z	B, Å²
N(1)	0.500	0.021 (1)	0.250	5.3 (9)*	Co(1)	0.6185 (3)	0.1092 (1)	0.2030 (3)	4.6 (1)
N(2)	0.850 (2)	0.1651 (8)	0.344 (2)	7.1 (7)*	Co(2)	0.5794 (3)	0.1839 (1)	0.2088 (4)	5.9 (1)
N(3)	0.605 (4)	0.162 (1)	−0.023 (4)	6 (1)*	P(1)	0.4324 (7)	0.1369 (3)	0.1425 (7)	5.1 (2)
C(1)	0.500	−0.025 (2)	0.250	9 (2)*	P(2)	0.6043 (8)	0.0474 (3)	0.2198 (8)	5.6 (3)
C(2)	0.976 (3)	0.172 (1)	0.424 (4)	9 (1)*	P(3)	0.7977 (8)	0.1180 (3)	0.2974 (9)	7.7 (3)
C(3)	0.575 (6)	0.170 (2)	−0.178 (7)	9.0*	P(4)	0.7498 (8)	0.2013 (3)	0.2991 (9)	8.1 (3)
C(4)	0.500	0.227 (1)	0.250	6 (1)*	P(5)	0.631 (2)	0.1165 (7)	0.034 (1)	6.9 (5)
C(5)	0.331 (3)	0.1303 (9)	−0.015 (3)	5.6 (8)*	P(6)	0.572 (2)	0.2005 (6)	0.046 (2)	8.6 (6)
C(6)	0.305 (3)	0.091 (1)	−0.065 (3)	7 (1)*	F(1)	0.713 (2)	0.0239 (6)	0.303 (2)	8.5 (5)*
C(7)	0.224 (3)	0.081 (1)	−0.184 (4)	9 (1)*	F(2)	0.600 (2)	0.0210 (6)	0.103 (2)	8.0 (5)*
C(8)	0.167 (3)	0.112 (1)	−0.244 (4)	10 (1)*	F(3)	0.879 (2)	0.1021 (8)	0.233 (2)	11.6 (7)*
C(9)	0.175 (3)	0.154 (1)	−0.209 (4)	10 (1)*	F(4)	0.865 (2)	0.0917 (6)	0.417 (2)	9.6 (6)*
C(10)	0.258 (3)	0.160 (1)	−0.095 (3)	8 (1)*	F(5)	0.814 (2)	0.2292 (7)	0.236 (2)	10.2 (6)*
C(11)	0.629	0.117	0.029	8.0*	F(6)	0.799 (2)	0.2283 (7)	0.423 (2)	9.8 (6)*
C(12)	0.569	0.201	0.039	8.0*	F(7)	0.767 (3)	0.107 (1)	0.032 (3)	8 (1)*
H(6)	0.3472	0.0690	−0.0154	9*	F(8)	0.569 (3)	0.094 (1)	−0.069 (3)	5.8 (9)*
H(7)	0.2139	0.0537	−0.2165	9*	F(9)	0.667 (3)	0.236 (1)	0.038 (4)	9 (1)*
H(8)	0.1092	0.1075	−0.3240	9*	F(10)	0.481 (3)	0.221 (1)	−0.054 (3)	6.4 (9)*
H(9)	0.1277	0.1744	−0.2569	9*	O(4)	0.500	0.263 (1)	0.250	7.5 (9)*
H(10)	0.2718	0.1880	−0.0623	9*	O(11)	0.636	0.121	−0.066	8.0*
					O(12)	0.562	0.210	−0.058	8.0*

[a] Anisotropically refined atoms are given in the form of the isotropic equivalent thermal parameter defined as $^4/_3[a^2B_{11} + b^2B_{22} + c^2B_{33} + ab(\cos\gamma)B_{12} + ac(\cos\beta)B_{13} + bc(\cos\alpha)B_{23}]$. Values marked with asterisks identify atoms refined isotropically.

a Princeton Applied Research (PAR) Model 175 universal programmer. Bulk electrolysis experiments were carried out with a PAR 173 potentiostat/galvanostat equipped with a PAR 179 digital coulometer, which provided a feedback compensation for ohmic drop between the working and reference electrodes. The voltage-follower amplifier (PAR 178) was mounted external to the potentiostat with a minimum length of high-impedance connection to the reference electrode. A 0.1-μF capacitor was connected between the voltage-follower amplifier lead and the counter electrode to ensure low noise pickup. Cyclic voltammetric profiles were displayed on a Tektronix 5115 storage oscilloscope or recorded directly on a Houston Series 2000 X-Y recorder. Pollution of the electrodes was not apparent in these studies. Solution aging was also undetected, since we were able to reproduce the potential/current profiles throughout the course of an experiment. The platinum-disk CV working electrode was periodically polished with a very fine emery cloth.

The cyclic voltammetric and bulk electrolysis cells were of airtight design with high-vacuum Teflon valves (Kontes) and Viton O-ring seals to allow an inert atmosphere to be maintained without contamination by grease.[12] The adjustable platinum CV working electrode was embedded in a cobalt-glass seal to allow periodic polishing without significantly changing the surface area. The working electrode used in the bulk electrolysis studies consisted of a platinum-wire cage wrapped with platinum gauze for a total surface area of ~1.1 cm². The SCE reference and saturated-KCl salt bridge were separated from the solution by a cracked-glass tip. The counter electrode for the CV studies, consisting of a platinum gauze, was separated from the working electrode by less than 2 mm and was connected to the reference electrode via a 0.1-μF capacitor to assist in the compensation for *iR* drop. The counter electrode used in the bulk electrolysis experiments was constructed from a double coil of nichrome wire possessing a large surface area. The standard oxidation and reduction potentials for the tetracobalt clusters in Table IV was determined by cyclic voltammetry. They were evaluated from the anodic (E_p^a) and cathodic (E_p^c) peak potentials.[33]

Bulk Electrolytic Reduction of $Co_4(CO)_{10}(PPh)_2$ in the Presence of $(F_2P)_2NMe$. To an argon-flushed bulk electrolysis cell was added 0.53 g (0.72 mmol) of $Co_4(CO)_{10}(PPh)_2$ and 40 mL of THF containing 0.3 M TBAP. After brief stirring, 0.12 mL (~0.72 mmol) of $(F_2P)_2NMe$ was added and the electrolysis initiated. The bulk electrolysis was conducted at room temperature in the constant-potential mode at −1.1 V as previously described.[12] However, the electrode potential did not diminish as expected for an electrocatalytic ECE substitution process. After passage of 1.05 C (~4 h) the reaction solution was examined by IR analysis, which revealed that only 10% of the starting cluster was present. At this point the reaction solution was reoxidized at 0.0 V until 0.84 C was passed and the current fell to zero. The crude reaction mixture was again examined by IR analysis, which suggested the presence of $Co_4(CO)_8(PPh)_2[(F_2P)_2NMe]$ as the major product in the reaction mixture. It was subsequently isolated by column chromatography over silica gel using hexane to afford ~0.2 g of a red-black solid. The structure was assigned as $Co_4(CO)_8(PPh)_2[(F_2P)_2NMe]$ on the basis of spectroscopic analysis (vide infra). Attempts to grow single crystals of the product suitable for X-ray diffraction were unsuccessful and afforded only a fine microcrystalline powder. IR (hexane; ν_{CO}, cm⁻¹): 2061 (m), 2041 (vs), 2029 (vs), 2019 (vs), 2011 (m), 1881 (m). $^{31}P\{^1H\}$ NMR ($CDCl_3$, 25 °C): δ 160.0 (b t, μ_4-PPh and fluorophosphine). ^1H NMR ($CDCl_3$, 25 °C): δ 2.20 (3 H, methyl), 7.4 (10 H, b).

X-ray Diffraction Study of $Co_4(CO)_3(PPh)_2[(F_2P)_2NMe]_4$. A large dark purple parallelepiped, approximate dimensions 0.50 × 0.50 × 0.60 mm, was mounted on an Enraf-Nonius CAD-4 automatic diffractometer. The crystal was of very poor quality, having wide ω scans, and did not scatter our very far in 2θ despite the large volume of the sample. The radiation used was Mo Kα monochromatized by a dense graphite crystal assumed for all purposes to be 50% imperfect. The Laue symmetry was determined to be 2/*m*, and the space group was shown to be either *C*2/*c* or *Cc*. Intensities were measured by the use of the θ–2θ scan technique, with the scan rate depending on the net count obtained in rapid prescans of each reflection. Two standard reflections were monitored periodically during the course of the data collection as a check of the crystal stability and the electronic reliability. These showed a 7% decay over 107 h. A linear correction was applied to account for this decay. In reduction of the data, Lorentz and polarization factors were applied, as well as an empirical absorption correction based on azimuthal ψ scans of five reflections having χ near 90°.[51] The structure was solved by MULTAN,[52] which showed 2 Co and 6 P atoms in the half-molecule of the asymmetric unit in space group *C*2/*c*. After we concluded that the molecule seemed to possess five fluorophosphine ligands, the refinement improved. However, there were still problems with the temperature factors and positions of two of the ligands related by the 2-fold axis around which the molecule is situated. The space group was thus changed to *Cc*, and the problems persisted. The cause was finally traced to disorder between two carbonyls, which replaced one bridging ligand part of the time at two sites related by a 2-fold axis in *C*2/*c*. Since the disorder remained in the *Cc* refinement, we decided to return to *C*2/*c* and finish the least squares. When the thermal parameters of the afflicted P atoms were fixed close to those of the remaining P atoms, the disorder was found to be almost exactly 50%, thus indicating a tetrasubstituted complex. This true disorder now explained the poor quality and low scattering power of the data crystal. The Co and P thermal parameters were converted to anisotropic values, and ideal hydrogens were added onto the phenyl ring. No sign of the methyl hydrogens appeared in difference Fourier syntheses, and thus no attempt was made to position them ideally. After all shift/esd ratios were less than 0.1, the full-matrix least squares converged at the agreement factors listed in Table I. Anomalous dispersion coefficients for the heavier elements were included. No unusually high correlations were noted between any of the variables in the last cycle of least-squares refinement. The final difference density map was featureless. All calculations were made by using Molecular Structure Corp.'s TEXRAY 230

(51) North, A. C. T.; Phillips, D. C.; Mathews, F. S. *Acta Crystallogr., Sect. A: Cryst. Phys., Diffr., Theor. Gen. Crystallogr.* **1968**, *A24*, 351.

(52) Germain, G.; Main, P.; Woolfson, M. M. *Acta Crystallogr., Sect. A: Cryst. Phys., Diffr., Theor. Gen. Crystallogr.* **1971**, *A27*, 368.

modifications of the SDP-PLUS series of programs.

Bulk Coulometry and EPR Studies of Fluorodiphosphine Clusters II and III. To determine the number of electrons involved in each redox couple of clusters II and III, the bulk coulometric measurements were generally performed as described in detail for the pentakis derivative III. To an argon-flushed cell for bulk electrolysis was added 0.107 g (0.08 mmol) of $Co_4(CO)(PPh)_2[(F_2P)_2NMe]_5$ and 35 mL of THF containing 0.3 M TBAP. The 0/+1 redox couple was first examined by constant-potential electrolysis at +1.0 V vs. SCE and 25 °C. The current gradually diminished as the electrolysis proceeded (total time ~1 h). No current flow was observed after passage of 7.91 C (theoretical value 7.85 C). This afforded a value of $n = 1.01$, consistent with the proposed redox couple as a one-electron oxidation process. At this point, a small aliquot of the electrolysis solution was examined by EPR spectroscopy. However, the solution was EPR-silent. The solution was reduced back to the neutral starting cluster at a potential of 0.0 V vs. SCE at 25 °C. Reduction of the radical cation to III required 7.53 C and afforded a value of $n = 0.95$. Next, the neutral solution of III was reduced to its radical anion at a potential of −1.5 V vs. SCE in the constant-potential mode. After the passage of 7.91 C, the current flow ceased, which afforded a value of $n = 1.05$ for the 0/−1 redox couple. EPR analysis of the radical anion solution was negative. The absence of EPR signals in these type of clusters has also been previously noted. This situation may arise from the cobalt cluster, which is composed of Co(II).[53] Such Co(II) complexes are known to relax rapidly, which generally precludes the EPR resonances under normal conditions ($T > 77$ K). Finally, the radical anion was reoxidized to the neutral III at a potential of 0.0 V vs. SCE to yield a value of $n = 0.63$. This suggested that some material loss had occurred. Similar experiments were performed with II to afford values of $a = 1.05$ (0/+1 couple) upon oxidation and $n = 0.79$ for reduction of the radical cation back to the neutral II. Reduction of II to the radical anion led to $n = 0.93$, and reoxidation of the radical anion to II yielded $n = 0.66$. As in cluster III, solutions of both the radical cation and the radical anion derived from II were EPR-silent.

Acknowledgment. We thank Dr. R. Hoffmann for helpful correspondence, Dr. J. Korp for the crystallographic determination, and the National Science Foundation and the Robert A. Welch Foundation for financial support.

Supplementary Material Available: Lists of bond lengths, bond angles, and general temperature factor expressions of the fluorophosphine and phenyl groups (5 pages); a list of structure factor amplitudes (5 pages). Ordering information is given on any current masthead page.

(53) (a) Orton, J. W. *Electron Paramagnetic Resonance*; Iliffe: London, 1968. (b) Carrington, A.; McLachlan, A. D. *Introduction to Magnetic Resonance*; Wiley: New York, 1979.

Contribution from the Department of Chemistry, University of Western Ontario, London, Ontario, N6A 5B7 Canada

Phthalocyanine π-Cation-Radical Species: Photochemical and Electrochemical Preparation of $[ZnPc(-1)]^{\bullet+}$ in Solution

Tebello Nyokong, Zbigniew Gasyna, and Martin J. Stillman*

Received May 21, 1986

The π-cation-radical species of ZnPc, $[ZnPc(-1)]^{\bullet+}$ (Pc = phthalocyanine), has been formed quantitatively as a stable product in solution following photochemical reactions with visible-region light in the presence of electron acceptors. The photolyses were carried out by excitation into the phthalocyanine's Q band ($\lambda > 580$ nm), with carbon tetrabromide as an irreversible electron acceptor. The neutral parent species could be regenerated following photooxidation by the addition of sodium dithionite. Cyclic voltammetry of neutral ZnPcL species identified the ring oxidation potentials; for ZnPc(py) and ZnPc(im) (py = pyridine; im = imidazole). In dimethylacetamide, there is one oxidation couple at 0.70 and 0.71 V vs. SCE, respectively, and there are two reduction couples, at −0.96 and −1.28 V vs. SCE, for the pyridine complex, and at −0.98 and −1.53 V vs. SCE, for the imidazole complex. Each of these reactions was reversible on the cyclic voltammetry time scale. The electrochemical and photochemical oxidation products were characterized by absorption, magnetic circular dichroism (MCD), and electron paramagnetic resonance (EPR) spectroscopies. Four clearly resolvable, optical transitions, centered at 440, 500, 720, and 825 nm, are observed in the absorption spectrum of the cation radical species. The MCD spectrum shows that the transition at 500 nm is nondegenerate, while the transitions at 440, 720, and 825 nm appear to be degenerate. EPR spectra obtained from frozen solutions of the π cation radicals gave isotropic g values that are characteristic of the oxidation at the phthalocyanine ligand (the g values were between 2.0055 and 2.0068).

Introduction

The phthalocyanines and porphyrins enjoy a growing importance as potential photo- and electrocatalysts for energy conversion processes,[1-5] as they are highly colored, exhibit diverse redox activity, and are relatively photochemically stable. Compared with the analogous porphyrin compounds, phthalocyanines are generally more resistant to ring degradation.[1] However, photochemical processes involving these ring compounds are only poorly developed, even though the chemistry of the excited states of molecules with so many π electrons is likely to be extensive. As part of our studies on the use of photochemically induced charge separation as the initial reaction step in a molecular solar cell,[6] we have examined the electrochemical and photochemical oxidation of zinc phthalocyanine (ZnPc) in solution.

Zinc phthalocyanines have been shown to exhibit photocatalytic properties, for example as photosensitizers for the reduction of methylviologens[7-9] and water.[10] It is known from cyclic voltammetry (CV) measurements that ZnPc undergoes chemical oxidation at the ring rather than at the metal center,[11] resulting in the formation of a phthalocyanine π cation radical on the CV time scale. Because of the very limited solubility of ZnPc in many nonpolar solvents, spectra of $[ZnPc(-1)]^{\bullet+}$ species have been

*To whom correspondence should be addressed.

(1) Darwent, J. R.; Douglas, P.; Harriman, A.; Porter, G.; Richoux, M. C. *Coord. Chem. Rev.* **1982**, *44*, 83.
(2) Lever, A. B. P.; Licoccia, S.; Ramaswamy, B. S.; Kadil, S. A.; Stynes, D. V. *Inorg. Chim. Acta* **1981**, *51*, 167.
(3) Ohtani, H.; Kobayashi, T.; Ohno, T.; Kato, S.; Tanno, T.; Yamada, A. *J. Phys. Chem.* **1984**, *88*, 4431.
(4) Kobayashi, T.; Nishiyama, Y. *J. Phys. Chem.* **1985**, *89*, 1167.
(5) Van Den Brink, F.; Visccher, W.; Barendrecht, E. *J. Electroanal. Chem. Interfacial Electrochem.* **1985**, *175*, 279.
(6) McIntosh, A. R.; Siemiarczuk, A.; Bolton, J. R.; Stillman, M. J.; Ho, T.-F.; Weedon, A. C. *J. Am. Chem. Soc.* **1983**, *105*, 7215.
(7) Darwent, J. R. *J. Chem. Soc., Chem. Commun.* **1980**, 805.
(8) Ohno, T.; Kato, S.; Lightin, N. N. *Bull. Chem. Soc. Jpn.* **1982**, *55*, 2753.
(9) Lever, A. B. P.; Licoccia, S.; Ramaswamy, B. S.; Kandil, S. A.; Stynes, D. V. *Inorg. Chim. Acta* **1981**, *51*, 169.
(10) Darwent, J. P.; McCubbin, I.; Phillips, D. *J. Chem. Soc., Faraday Trans. 2* **1982**, *78*, 347.
(11) Lever, A. B. P.; Licoccia, S.; Magnell, K.; Minor, P. C.; Ramaswamy, B. C. *Electrochemical and Spectrochemical Studies of Biological Redox Components*; Advances in Chemistry 201; American Chemical Society: Washington, DC, 1982; p 237.

0020-1669/87/1326-0548$01.50/0